# A New Enantiornithine (Aves) Preserved in Mid-Cretaceous Burmese Amber Contributes to Growing Diversity of Cretaceous Plumage Patterns

Lida Xing[1,2,3†], Jingmai K. O'Connor[4,5*†], Kecheng Niu[3], Pierre Cockx[6,7], Huijuan Mai[8,9] and Ryan C. McKellar[6,7,10]

[1] State Key Laboratory of Biogeology and Environmental Geology, China University of Geosciences, Beijing, China, [2] School of the Earth Sciences and Resources, China University of Geosciences, Beijing, China, [3] Yingliang Stone Nature History Museum, Nan'an, China, [4] Key Laboratory of Vertebrate Evolution and Human Origins, Chinese Academy of Sciences, Institute of Vertebrate Paleontology and Paleoanthropology, Beijing, China, [5] CAS Center for Excellence in Life and Paleoenvironment, Beijing, China, [6] Royal Saskatchewan Museum, Regina, SK, Canada, [7] Department of Biology, University of Regina, Regina, SK, Canada, [8] Yunnan Key Laboratory for Palaeobiology, Yunnan University, Kunming, China, [9] MEC International Laboratory for Palaeobiology and Palaeoenvironment, Yunnan University, Kunming, China, [10] Department of Ecology and Evolutionary Biology, University of Kansas, Lawrence, KS, United States

Recent discoveries of enantiornithine birds trapped in amber have decreased the lower size limit of members of this clade, increased their morphological diversity, and provided significant new data regarding their plumage. Here, we describe a new specimen that consists of the distal extremities of both forelimbs and hindlimbs. Size and morphology suggest the specimen represents an immature individual. Although the skeletal morphology is poorly preserved, the new specimen most probably represents a member of the Enantiornithes based on the sum of its preserved morphologies, including its small size, elongate penultimate pedal phalanges, and large recurved unguals. Based on the lengths of the metatarsals, the new specimen is even smaller than previously described enantiornithines that preserve these elements; however, the forelimb elements are longer than those in the only other specimen preserving comparable overlapping skeletal material. This is suggestive of a diversity of limb proportions in the Burmese enantiornithine fauna, similar to that observed in the Jehol avifauna, in which intermembral indices range from approximately 1 to 1.5. The wing appears to consist of eight primaries, less than that of neornithines, contributing to mounting data that suggests the flight apparatus of enantiornithines was unique from that of other basal birds and neornithines. The well-preserved flight feathers are ornamented with pale basal bands, further adding to the diversity of Cretaceous plumage patterns revealed by Burmese amber specimens.

Keywords: enantiornithes, remiges, flight feathers, plumage patterns, limb proportions, intermembral index, albian – cenomanian, mesozoic

# INTRODUCTION

Scientific understanding of Mesozoic birds has grown enormously over the past three decades (O'Connor et al., 2011). For the first two decades, new information primarily came from the rich Lower Cretaceous deposits in northeastern China that yield the celebrated Jehol Biota (Chang et al., 2003; Zhou et al., 2003). Although the diversity reported from these deposits continues to increase, specimens are heavily compressed, limiting and obscuring the morphological data they contain (Wang and Zhou, 2019; Wang et al., 2019). In 2016, the first avian skeletal remains preserved encased in Albian-Cenomanian age Burmese amber were described (Xing et al., 2016). Since these two partial wings were reported, two partial skeletons (Xing et al., 2017, 2018a), another partial wing (Xing et al., 2020), and three partial hindlimbs have been described (Xing et al., 2019a,b,c). Together, these have revealed new details of enantiornithine plumage, such as the bizarre body feathers present in hatchlings and the presence of enigmatic scutellate scale filaments (Xing et al., 2017), as well as previously unknown skeletal morphologies such as the bizarrely elongated third pedal digit of *Elektororis chenguangi* (Xing et al., 2019c).

Particularly with regards to skeletal remains, the quality of preservation varies depending on the unique taphonomic conditions of each individual specimen. These include differences in whether the bird was alive or dead when it became trapped in the amber, whether it was partially scavenged, and how long it took for the remains to be fully encapsulated in the resin. As a result, skeletal preservation varies from excellent (Xing et al., 2019a) to absent, as in one specimen that preserves only a mold of the soft tissues (Xing et al., 2019b).

The new piece of Burmese amber YLSNHM00813 is from the Angbamo site, Tanai Township, Myitkyina District, Kachin State of northern Burma (Myanmar). Biostratigraphic evidence suggests that Burmese amber dates back to the middle–upper Albian based on ammonites (Wright et al., 1996), Albian–Cenomanian based on palynology (Davies, 2001), or Cenomanian–Turonian based on arthropods (Grimaldi et al., 2002). Radiometric dating using U-Pb from zircons found in the volcanoclastic matrix surrounding the amber has refined this age, providing an absolute estimate of $98.8 \pm 0.6$ Ma (Shi et al., 2012). This means that these amber specimens help to fill an important gap between the well-known Early Cretaceous avifaunas from China and Spain that are Barremian to Aptian (Sanz and Ortega, 2002; Pan et al., 2013) and Late Cretaceous specimens from North and South America that range from the Coniacian to Maastrichtian (Chiappe, 1993; Atterholt et al., 2018).

The new specimen YLSNHM00813 preserves the distalmost portions of two forelimbs and two feet all belonging to the same individual making it one of the relatively more complete specimens known so far (**Figure 1**). Feathers associated with both forelimbs are also preserved. The amber piece measures $127.34 \times 88.04 \times 44.52$ mm, and weighs 284 g. We describe the skeletal and integumentary remains and compare them to previously described specimens.

# MATERIALS AND METHODS

## Micro-CT Scanning and 3D Reconstruction

YLSNHM00813 was scanned with an X-ray micro-CT: Xradia 520 Versa (Carl Zeiss X-ray Microscopy, Inc., Pleasanton, CA, United States) at the Yunnan Key Laboratory for Palaeobiology, Yunnan University, Kunming, China. Without scanning it is impossible to view the morphology of the skeletal elements obscured both by the preservation of soft tissue and the amber itself, which includes numerous inclusions. The entire piece was scanned with a beam strength of 50 kV/4W for 168 min, with a voxel size of 26.59 um. A total of 1,014 radiographs were registered in the scan and saved as TIFF stacks and used to reconstruct the specimen with the Amira 5.4 software (Visage Imaging, San Diego, CA, United States). The subsequent volume rendering and animations were performed using VG Studiomax 2.1 (Volume Graphics, Heidelberg, Germany) (**Supplementary Figures 1–4**). Final figures were prepared with Photoshop CS5 (Adobe, San Jose, CA, United States) and Illustrator CS5 (Adobe, San Jose, CA, United States).

## Terminology and Abbreviations

Osteological terminology primarily follows Baumel and Witmer (1993) using the English equivalents for the Latin terms, while plumage is described with the terminology of Lucas and Stettenheim (1972). Institutional abbreviations for specimens used as comparative material include: DIP – Dexu Institute of Palaeontology, Chaozhou, China, HPG – Hupoge Amber Museum, Tengchong City China; YLSNHM – Yingliang Stone Nature History Museum, Nan'an, China.

# RESULTS

## Skeletal Description

The new specimen YLSNHM00813 preserves the distal portions of both wings and hindlimbs, although most of the skeletal elements are poorly preserved due to various degrees of dissolution and decay, thus preventing detailed morphological observations (**Figure 1** and **Supplementary Figures 1–4**).

## Forelimbs

The left wing is the better preserved of the two (**Figures 1–3**). The distal epiphyses of the radius and ulna are preserved in articulation with the hand, which is complete and nearly in full articulation. The cortex of the ulna appears to be very thin and the element is hollow. The condyles on the ulna extend from the distal to caudal surface; the intercondylar sulcus is only weakly developed. The radius appears to have a ventral aponeurosis tubercle, which is bordered by the tendinal sulcus. Three free carpals are preserved; the largest is interpreted as the ulnare, which is preserved ventrocaudal to the ulna (**Figure 3A**). It is wedge-shaped with the thicker end oriented toward the metacarpals. The radiale, preserved between the radius and the alular metacarpal, is smaller (approximately one-third the size
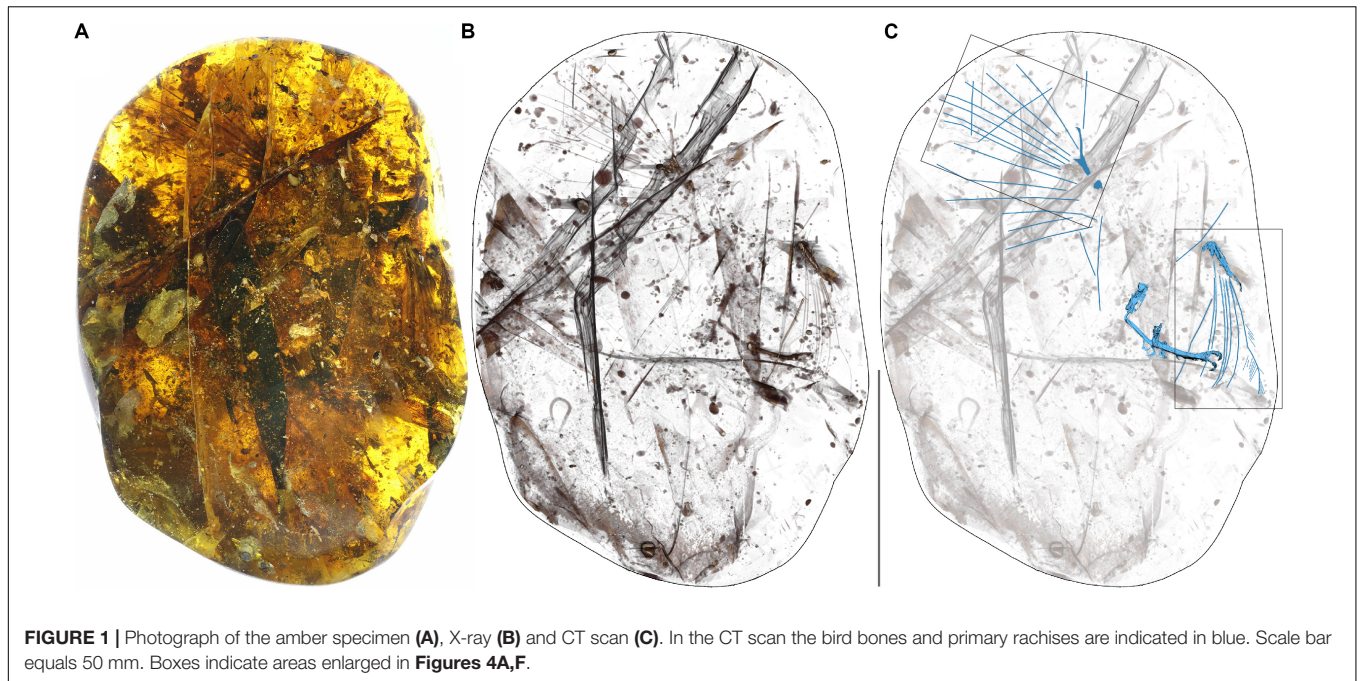
**FIGURE 1 |** Photograph of the amber specimen **(A)**, X-ray **(B)** and CT scan **(C)**. In the CT scan the bird bones and primary rachises are indicated in blue. Scale bar equals 50 mm. Boxes indicate areas enlarged in **Figures 4A,F**.

of the alular metacarpal), has a blunt triangular shape in profile, and is dorsoventrally compressed. The third carpal appears to be "carpal x" (Chiappe et al., 2007) and is preserved at the proximal end of the minor metacarpal, level with the major metacarpal such that the minor metacarpal is displaced distally. It is wedge-shaped, with the tapered end directed toward the minor metacarpal. The proximal end is dorsoventrally thicker than the distal end.

The alular digit is slightly disarticulated away from the rest of the hand, so that the alular metacarpal is not preserved in contact with the major metacarpal, indicating that these two elements were unfused (**Figure 3A**). The alular metacarpal is roughly rectangular, about twice as tall craniocaudally as it is dorsoventrally wide and 2.5 times as long as it is tall. The first phalanx of the alular digit is proximally robust and tapers distally, so that the craniocaudal thickness is twice proximally what it measures distally; it is more than twice the length of the alular metacarpal. The alular ungual phalanx is curved and dorsoventrally compressed, measuring nearly the same length as the alular metacarpal. Were the alular digit in articulation, it would extend distally to the level of the distal margin of the major digit.
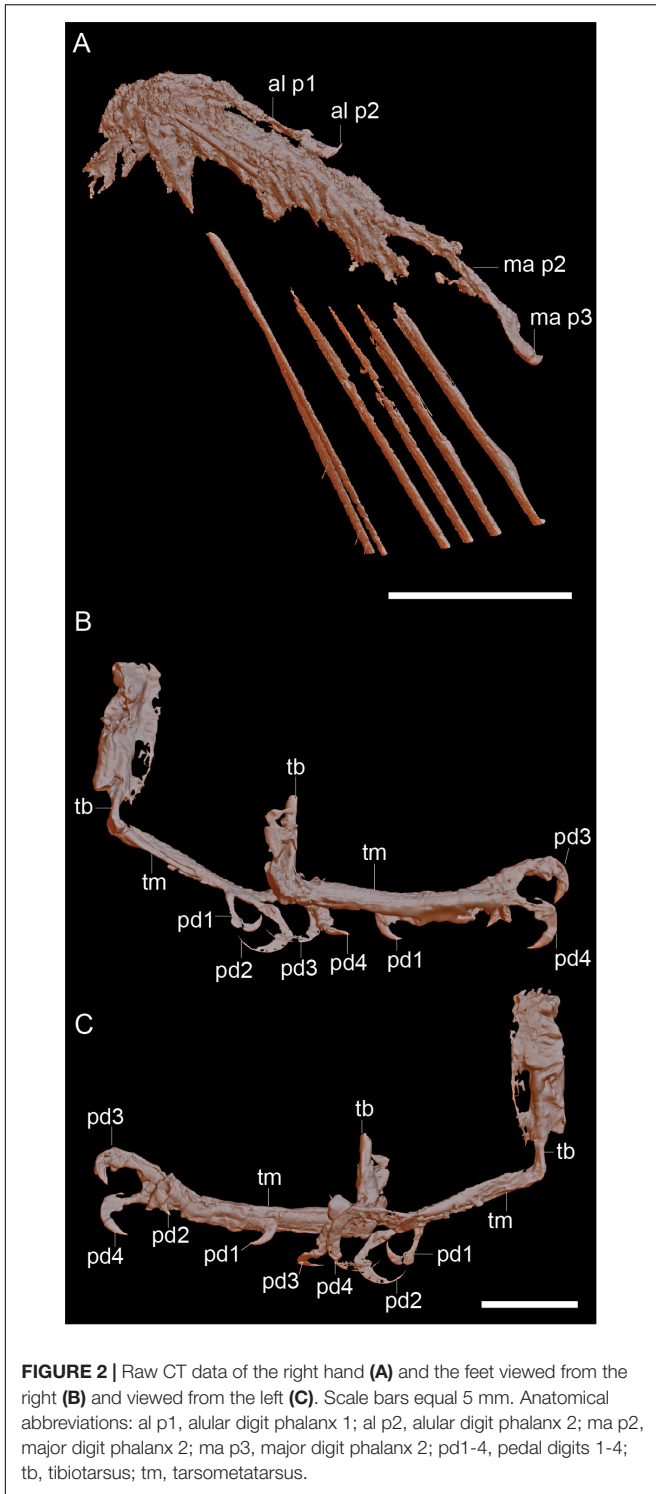
The proximal end of the major metacarpal is thickened relative to the shaft, especially in the dorsal direction (**Figure 3A**). It is possible the semilunate carpal was fused to the major metacarpal. Otherwise, this element is not preserved. The shaft of the major metacarpal is only slightly more robust than that of the minor metacarpal. As preserved, the two bones end distally at the same level. The distal end of the major metacarpal is weakly ginglymous. The major digit consists of three phalanges; the two non-ungual phalanges are roughly equal in length although the proximal phalanx is the longest. The major digit ungual phalanx is much larger than that of the alular digit, recurved, and with

a well-developed flexor tubercle. The articulations between the major digit phalanges appear to all be weakly ginglymous.

The highly reduced minor digit consists of two small phalanges, both strongly dorsoventrally compressed. The first is rectangular in profile and nearly twice as long as the second, which is triangular and sharply tapered distally (**Figure 3A**).

## Hindlimbs

The two hindlimbs are poorly preserved (**Figures 2B,C**). Morphological details can be best observed on the left limb (**Figure 3B**). The left hindlimb preserves the distal half (or more) of the tibiotarsus and the nearly complete foot in full articulation. The right preserves approximately the distal one-third of the tibiotarsus in articulation with the foot. The exposed cross section of the tibiotarsus shows the bone had thin cortical walls and was hollow. Soft tissue obscures the tibiotarsus and tarsometatarsus so that very few morphological details can be gleaned. The proximal tarsals appear to be fused to the tibia, but this is most likely an artifact due to poor preservation, given that the carpal bones are unfused. It appears the distal end of the tibiotarsus is expanded slightly relative to the shaft and slightly bowed cranially (**Figure 3B**). The latter morphology may be a product of poor preservation (the potentially unfused proximal tarsals may be deflected cranially beneath the soft tissue). The tarsometatarsus is proportionately long and narrow. The metatarsals are clearly unfused to each other on the right limb, although they are preserved in tight articulation on the left. The first metatarsal is preserved on the plantar surface of the tarsometatarsus, but it may be displaced. It is approximately 20% of the length of metatarsal III, as in most enantiornithines with the exception of the Pengornithidae (Wang et al., 2014). Metatarsal III is the longest, followed by metatarsal II and metatarsal IV, the latter of which is the shortest of the

FIGURE 2 | Raw CT data of the right hand **(A)** and the feet viewed from the right **(B)** and viewed from the left **(C)**. Scale bars equal 5 mm. Anatomical abbreviations: al p1, alular digit phalanx 1; al p2, alular digit phalanx 2; ma p2, major digit phalanx 2; ma p3, major digit phalanx 2; pd1-4, pedal digits 1-4; tb, tibiotarsus; tm, tarsometatarsus.



FIGURE 3 | Reconstruction of the right hand **(A)** and the left foot **(B)**. Scale bars equal 5 mm. Anatomical abbreviations not listed in the **Figure 2** caption: al, alular metacarpal; ma, major metacarpal; mi, minor metacarpal; ma p1, major digit phalanx 1; mi p1, minor digit phalanx 1; minor digit phalanx 2; ra, radius; rl, radiale; ul, ulna; un, ulnare.

three. The trochleae are narrow, not expanded relative to the metatarsal shafts.

The pedal phalangeal formula is 2-3-4-5-x. The third digit is the longest, closely followed by the fourth digit. The hallux is preserved in a fully reversed position in both the right and the left feet (**Figures 2B,C**). The first digit is short, with the
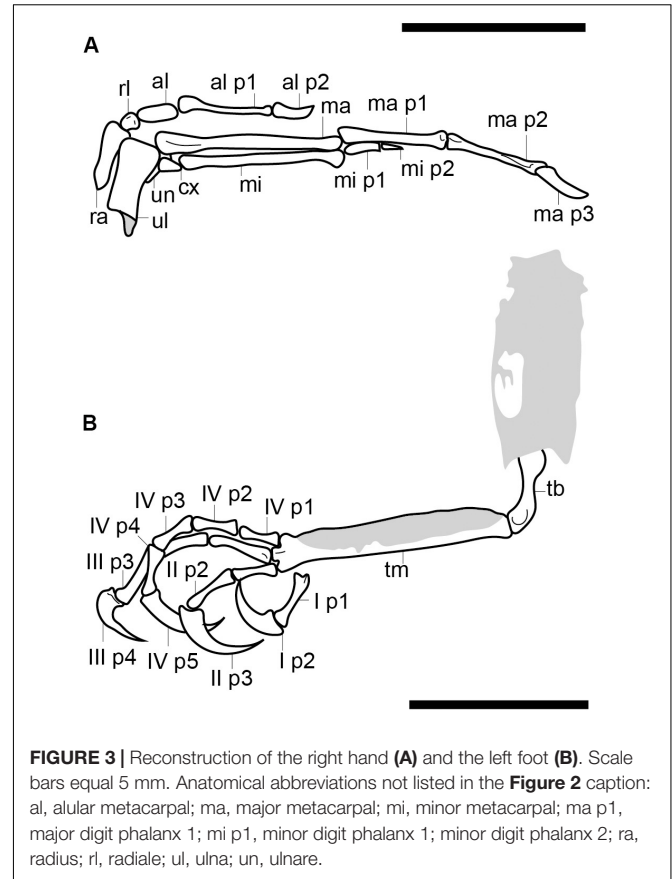
first phalanx similar in length to the claw, which is curved and sharply tapered with a small but distinct flexor tubercle. The first phalanx of the second digit is shorter than the penultimate phalanx, which is subequal to the first phalanx in the hallux but slightly more delicate. The second digit claw is longer and more robust (although it is slightly less recurved) than that of the hallux. The keratinous sheath remains in articulation on the pedal claws. The first phalanx of the third digit is the longest in the foot and subequal in length to the penultimate phalanx of the same digit. The second phalanx is approximately 75% the length of the preceding and following phalanges. The ungual phalanx of the third digit is larger, more robust, and more recurved than that of the second digit. The first phalanx of the fourth digit is the shortest in the foot. The following two phalanges are subequal in length and shorter than the penultimate phalanx. The claw is slightly smaller and less recurved that those of digits I–III (**Figure 3B**).

## Ontogeny and Taxonomy

So far, only enantiornithines have been unequivocally recovered from the Hukwang avifauna. The very small body size and unfused proximal carpometacarpus suggest that YLSNHM00813 is an immature individual. Similar to the immature holotype of *Iberomesornis romerali* (Sanz and Ortega, 2002), the minor metacarpal does not project farther distally than the major metacarpal as it does in most of the other enantiornithines

(Chiappe and Walker, 2002). Given the preservational state of the left manus, in YLSNHM00813 it is possible that this morphology is due to slight disarticulation of the metacarpals. The two non-ungual phalanges of the major digit are subequal, whereas in most enantiornithines the penultimate phalanx is shorter than the proximal one. The penultimate phalanx is longer in the basalmost enantiornithine *Protopteryx* (Zhang et al., 2001) and notably, the minor metacarpal only projects slightly farther than the major metacarpal in this taxon as well (Chiappe et al., 2019). The pedal phalanges are elongated distally so that the penultimate phalanx is the longest in each digit, as in all known enantiornithines. The claws are large and recurved as in all known enantiornithines, whereas in Cretaceous ornithuromorphs the pedal claws are short and unrecurved (O'Connor, 2012). Based on these morphological characteristics, the most parsimonious inference is that YLSNHM00813 represents an immature and fairly basal enantiornithine.

## Integument

Feathers from both the right and left wing are preserved, including what is interpreted as the complete set of primaries on both sides (**Figures 1, 4**). The left wing preserves eight primaries and four secondaries, with the two feather tracts separated by a small gap (**Figure 4A**). The primaries are truncated apically by the polished surface of the amber (**Figures 4B–E**). The exposed cross-sections of the primary rachises are subcylindrical basally and ovoid distally and are hollow and pith filled. The ventral rachis margins are slightly wider than the dorsal margins. The blade-shaped barb rami are deep (extending ventrally from the barbules) and dorsolaterally attached along the rachis (**Figures 4B,C**). Both the rachises and the barbs are preserved with a dark gray color due to pyrite infiltration. Proximal barbules are straight and blade-shaped, whereas the distal barbules have a slightly angled pennulum with hooklets that is poorly distinguished from the base. Primaries are strongly asymmetric, with barbs in the leading vane being approximately 0.4 times the length of the barbs in the trailing vane. Furthermore, the barbs differ in the angle of divergence from the rachis forming an angle of approximately 17° (standard error of about 0.66) in the leading-edge vane, versus approximately 28° (standard error of 0.98) in the trailing-edge vane.

In cross-section, the rachises of the secondaries are subcircular and are hollow and pith filled. Although less clear, it appears that the secondaries were also asymmetric, but less so than observed in the primary remiges (ratio of about 0.7). Primary coverts are sparsely preserved. They are short, restricted to the very base of the primaries. No secondary coverts can be identified but this region of the wing does not appear to be preserved.

The right wing also consists of eight primaries, together with three alular coverts and a sparse row of primary coverts (**Figure 4F**). The sparse distribution of the primary coverts in both wings is interpreted as due to taphonomic loss. Some feathers have been displaced and damaged (e.g., one secondary remex is strongly displaced anterior to the leading edge of the wing). Coverts from either the leading edge of the manus or the propatagium are preserved as a clump that has been offset ventral to the wing.
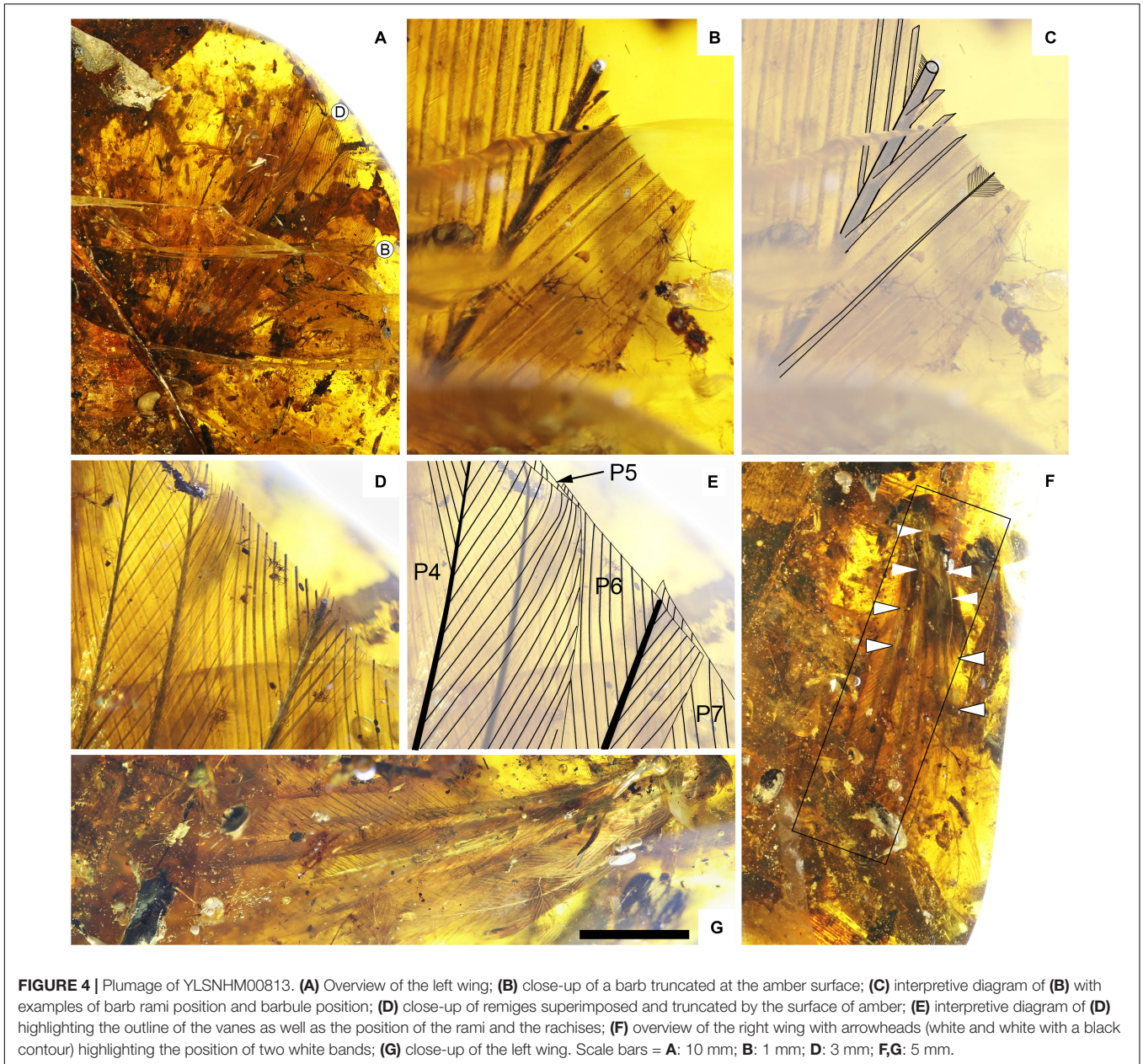
The right wing is structurally consistent with the left, but with slightly better visibility through the amber allowing better observation of color. In the right wing, the preserved primaries and coverts have pale rachises and barb rami. The barbules are medium brown with a grayish tinge. A pale band extends transversely along the basal quarter of the primary remiges and in the primary coverts (**Figure 4F**). A second pale band extends transversely across the primary coverts and partly into the alular coverts. The coverts are preserved with a darker brown coloration (**Figures 4F, 5A**).

CT-scan data show three rows of scutellae on the dorsal surface of the right leg (**Figure 2B**). No scutes are present. It was not possible to observe if scutellate scale filaments are present due to the delicate nature of these features and the large amount of overlapping plant material also trapped in the amber in YLSNHM00813 (**Figure 1A**).

## Taphonomy

The decay products and breaks within the preserved material suggest that the bird fell into the resin with its belly up, and that the dominant taphonomic processes were decay and drift (no signs of predation or scavenging). YLSNHM00813 is dominated by a scatter of large, strap-like leaves that are more than twice the size of the primary flight feathers (**Figure 1A**). The surrounding amber is also rich in wood particulates, plant detritus, insect frass, and contains representatives of multiple orders of arthropods (e.g., Coleoptera, Diptera, Hemiptera, Hymenoptera, Araneae, and Blattoidea), including forest floor dwelling groups, such as Diplopoda and Collembola. Altogether, this evidence suggests the resin mass formed on or near the forest floor, capturing a litter assemblage (Perrichot, 2004). Visibility is restricted by a combination of plant material on the dorsal side of the avian inclusion, and thick overlying amber full of particulates and fractures on the ventral surface. However, the dorsal surfaces of the wings are clearly visible, along with an assortment of detached feathers that are adrift within the resin flow. It may be a function of limited visibility, but no sheets of skin are visibly present within the amber mass, and most of the covert feathers that surround the primaries and secondaries appear to have been lost in the surrounding resin.

The preserved distal portions of the forelimbs are generally in the correct anatomical orientation, but they appear to have drifted relative to one another (**Figure 1A**). The jagged and irregular margins of the broken edges of the right radius and ulna suggest that these breaks occurred postmortem. Combined with the high number of isolated contour feathers in seemingly random orientations, the fractures and limb displacements indicate a high degree of decay and resin mobility before the limbs were fully engulfed and the resin began to polymerize. Bubbles emanating from the broken ends of bones, as well as those emanating from decaying plant material, have risen toward the ventral surface of the bird inclusion. Bent feathers and plant material indicate that the surrounding resin flowed toward the right side of the bird. Together, these observations indicate that the bird fell into the resin mass with its ventral surface exposed upward, where it proceeded to decay and weather extensively. The limbs were the only parts of the body deeply entombed in the

**FIGURE 4 |** Plumage of YLSNHM00813. **(A)** Overview of the left wing; **(B)** close-up of a barb truncated at the amber surface; **(C)** interpretive diagram of **(B)** with examples of barb rami position and barbule position; **(D)** close-up of remiges superimposed and truncated by the surface of amber; **(E)** interpretive diagram of **(D)** highlighting the outline of the vanes as well as the position of the rami and the rachises; **(F)** overview of the right wing with arrowheads (white and white with a black contour) highlighting the position of two white bands; **(G)** close-up of the left wing. Scale bars = **A**: 10 mm; **B**: 1 mm; **D**: 3 mm; **F,G**: 5 mm.

resin, leading to their preferential preservation and subsequent drift within the fluid resin. The limbs do not have a heavy coating of milky amber surrounding them, and the skin around the feet adheres tightly to the underlying bones. This likely indicates that the body parts dried on the surface prior to encapsulation, but it is possible that decay products may have been swept away from the feet by resin flows (Martínez-Delclòs et al., 2004).

## DISCUSSION

The specimen described here, YLSNHM00813, is the ninth reported Burmese amber specimen preserving avian skeletal remains. Although the skeletal remains are poorly preserved,

the cumulative morphological features (e.g., penultimate pedal phalanges longest, pedal ungual phalanges long and recurved) suggest referral to the Enantiornithes, the dominant clade of Cretaceous land birds (O'Connor et al., 2011) and so far the only clade identified with certainty in Burmese amber (Xing et al., 2016, 2017, 2018a, 2019a,b,c). The position of the forelimbs and hindlimbs in the amber block suggests that these remains belong to a single individual (**Figure 1**). As in other specimens thus far preserved in amber, YLSNHM00813 is very small with the metatarsals measuring less than one centimeter (**Table 1**). The only specimen in which both forelimb and hindlimb measurements can be compared is the hatchling HPG-15-1 (Xing et al., 2017). Compared to HPG-15-1, the foot is slightly smaller in YLSNHM00813, yet the hand is larger (**Table 1**). This suggests
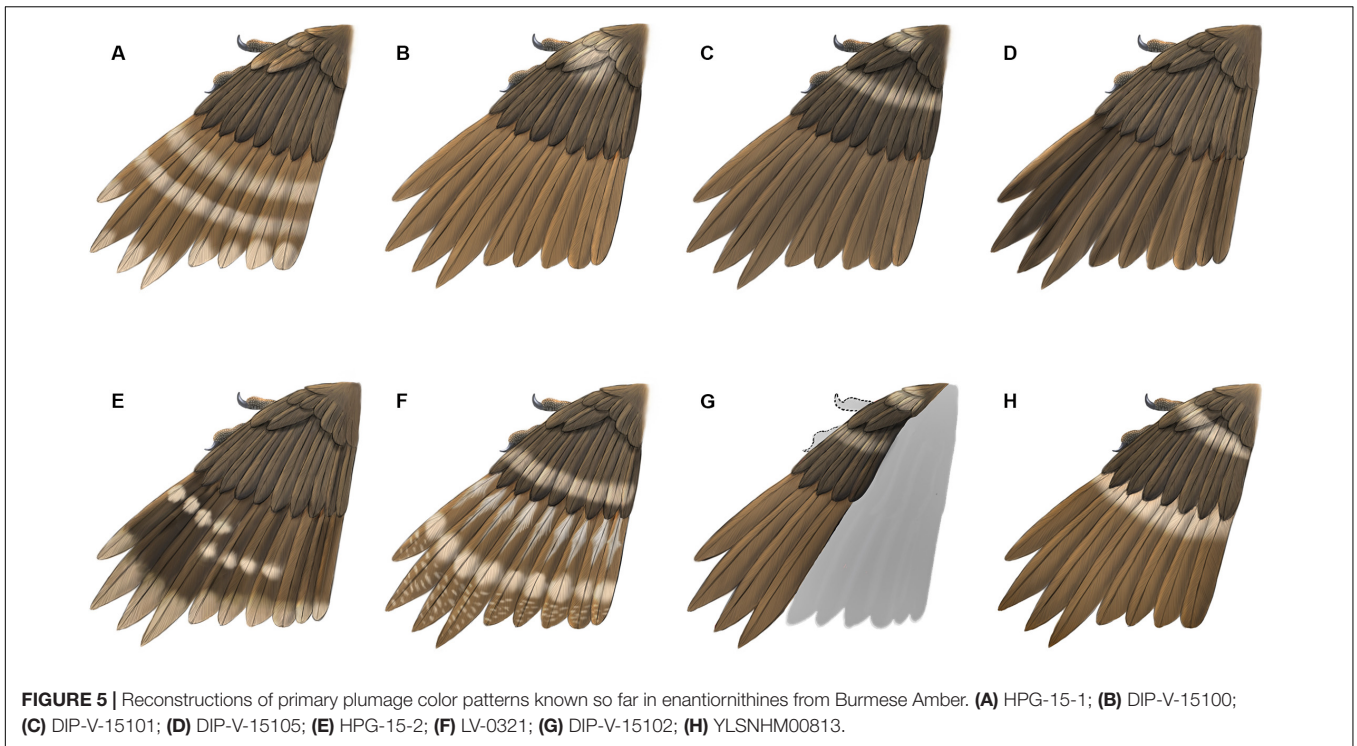
**FIGURE 5 |** Reconstructions of primary plumage color patterns known so far in enantiornithines from Burmese Amber. **(A)** HPG-15-1; **(B)** DIP-V-15100; **(C)** DIP-V-15101; **(D)** DIP-V-15105; **(E)** HPG-15-2; **(F)** LV-0321; **(G)** DIP-V-15102; **(H)** YLSNHM00813.

that YLSNHM00813 would have had a higher intermembral index and proportionately larger wingspan than HPG-15-1. Such diversity is unsurprising: enantiornithines from the Jehol avifauna show considerable variation in limb proportions, with species ranging from subequal forelimbs and hindlimbs (e.g., *Monoenantiornis*, *Rapaxavis*) to taxa with forelimbs considerably elongated relative to the hindlimbs (e.g., *Longipteryx, Pengornis*) (O'Connor et al., 2009; Hu and O'Connor, 2017). Mesozoic birds with elongated hindlimbs are so far only definitively known in the Ornithuromorpha (O'Connor et al., 2010). Differences in limb proportions between Burmese amber enantiornithines likely reflect subtle ecological differences between species. The better preserved and more complete specimen HPG-15-1 has been interpreted as a hatchling, and YLSNHM00813 is also likely an immature individual, as suggested by the apparently unfused proximal carpometacarpus (**Figure 3A**).

The primary wing feathers are well preserved in YLSNHM00813. The number of preserved primaries is eight on both sides, which suggests the tract is complete (**Table 2**). Eight remiges are also preserved in HPG-15-1, but it is unclear if the tract is complete in the latter specimen (Xing et al., 2017). Nine primaries are preserved in DIP-V-15100, which also preserves secondaries and thus is likely complete (Xing et al., 2016), and ten primaries are reported in DIP-V15105 (Xing et al., 2019a). Specimen HPG-15-2 may have ten or perhaps 11 primaries, but it is difficult to distinguish between the primaries and secondaries due to feather overlap within this specimen (Xing et al., 2019c). When wings are preserved, the number of primary feathers usually cannot be accurately estimated in lithic specimens due to overlap but in amber specimens the remige count is aided by CT data that clearly reveals the rachis of each

flight feather. The data from the Hukawng avifauna indicates intraclade diversity in the number of primary feathers in the wing in enantiornithines, as in neornithines (Gill, 2007). This diversity hints at potential differences in wing shape and flight style between species. In neornithines the number of primaries ranges from nine to 12 (Lovette and Fitzpatrick, 2004); *Archaeopteryx* falls in the modern range with 11 primaries (Elzanowski, 2002). Currently available data suggests the number of primaries in enantiornithines ranged from eight to 11. This contributes to the numerous lines of evidence that the flight apparatus of enantiornithines was unique from that of other basal birds and neornithines (Chiappe and Walker, 2002). The rest of the wing plumage in YLSNHM00813 is poorly preserved due to extensive postmortem decay. The most valuable information lies in the preserved coloration, adding to the known diversity of plumage patterns recognized among Mesozoic birds.

## Diversity of Plumage Patterns

As specimens accumulate so has the diversity of plumage color patterns observed in enantiornithines in Burmese amber (**Figure 5** and **Table 2**). Although in very rare instances patterns such as stripes and spots are preserved directly in some lithic specimens (Chen et al., 1998; Ji et al., 1998; de Souza Carvalho et al., 2015; Zheng et al., 2017; Li et al., 2018), these do not necessarily reflect color differences and may indicate areas of increased melanization (Zheng et al., 2017). It is possible to determine the original melanosome-based coloration in well preserved lithic fossils by sampling the preserved traces and viewing them using a scanning electron microscope (SEM) to look for preserved melanosomes; however, getting a clear picture of the entire wing coloration would require extensive destructive

**TABLE 1 |** Comparative measurements of enantiornithines from the Hukawng avifauna.

| | YLSNHM00813 | DIP-V-15100 | DIP-V-15101 | HPG-15-1 | DIP-V-15102 | YLSNHM01001 | DIP-V-15105a | HPG-15-2 | LV-0321 |
|---|---|---|---|---|---|---|---|---|---|
| Ulna | (2.55) | (7.94) | | (5.22) | 14.38 | | | | |
| Radius | (1.91) | (6.5) | | (5.48) | 12.93 | | | | |
| Alular metacarpal | 1.08 | 1.00 | | | | | | | |
| Alular phalanx-1 | 2.36 | 1.83 | (2.95) | 1.68 | | | | | |
| Alular phalanx-2 | 1.13 | 1.28 | 1.81 | 0.94 | | | | | |
| Major metacarpal | 5.2 | 4.17 | (4.95) | 3.88 | | | | | |
| Major phalanx-1 | 3.03 | 2.22 | 3.10 | 1.85 | | | | | (2.41) |
| Major phalanx-2 | 2.73 | 1.78 | 2.57 | 1.23 | | | | | 4.51 |
| Major phalanx-3 | 1.49 | 1.28 | 2.14 | 1.00 | | | | | 2.21 |
| Minor metacarpal | 4.55 | 4.72 | (6.24) | 3.85 | | | | | |
| Minor phalanx-1 | 1.09 | 1.00 | 1.38 | 1.07 | | | | | |
| Metatarsal I | | | | | | | 1.57 | 1.87 | |
| Metatarsal II | 6.95 | | | 7.50 | | | (2.67) | 6.75 | |
| Metatarsal III | 7.02 | | | 8.00 | | (5.2) | (2.39) | 7.55 | |
| Metatarsal IV | 6.71 | | | 7.17 | | | (2.29) | 6.97 | |
| Digit I-1 | 1.49 | | | | | | 2.17 | 2.95 | |
| Digit I-2 | 1.59 | | | | | | 2.57 | 1.71 | |
| Digit II-1 | 1.25 | | | | | | 1.20 | 1.24 | |
| Digit II-2 | 1.49 | | | | | | 2.44 | 2.31 | |
| Digit II-3 | 2.09 | | | | | 4.50 | 3.10 | 1.84 | |
| Digit III-1 | 2.02 | | | 2.10 | | | 1.57 | 1.97 | |
| Digit III-2 | 1.49 | | | | | | 1.56 | 2.35 | |
| Digit III-3 | 1.95 | | | | | | 2.04 | 2.95 | |
| Digit III-4 | 1.95 | | | | | | | 1.81 | |
| Digit IV-1 | 1.18 | | | | | | 0.84 | 0.98 | |
| Digit IV-2 | 1.32 | | | | | | 0.85 | 1.33 | |
| Digit IV-3 | 1.2 | | | | | | 0.91 | 1.24 | |
| Digit IV-4 | 1.35 | | | | | | 1.59 | 1.65 | |
| Digit IV-5 | 2.12 | | | | | | 1.36 | 1.78 | |

*Measurements represent lengths in mm; parentheses indicate incomplete elements. Measurements of pedal unguals do not include the keratinous sheath.*

**TABLE 2 |** Wing plumage characteristics in Hukawng enantiornithines.

| Collection No. | Publication | Ontogeny | Primaries | Secondaries | Plumage pattern |
|---|---|---|---|---|---|
| HPG-15-1 | Xing et al., 2017 | Hatchling | (8) | 9 | Each primary feather with walnut brown color with pale feather apex and two pale transverse bands in distal half. Single preserved alular feather with trailing edge paler than the leading edge. |
| DIP-V-15102 | Xing et al., 2018a | Juvenile | (4) | (10)/(11) | In primaries, barbules, rami and rachises all preserved a diffuse, pale brown color. |
| HPG-15-2 | Xing et al., 2019c | Subadult/Adult | 10/11 | 4/3 | Wing preserved overall dark brown color; two large-scale pale wing spots; barb apices in trailing edge vane of primaries pale or white. |
| DIP-V-15100 | Xing et al., 2016 | Juvenile | 9 | 5 | Overall dark brown coloration with pale or white spot basal to the alula, which extends on to some of the primary coverts |
| DIP-V-15101 | Xing et al., 2016 | Juvenile | 9 | (5) | Overall dark brown coloration with pale or white spot basal to the alula; second pale band present extending across the dorsal surface of the wing apical to the alula. |
| LV-0321 | Xing et al., 2020 | ? | 8/9 | – | Overall dark, walnut brown color; longitudinal pale stripe in basal half of each primary extending along the rachis; more diffuse transverse pale patch located subapically |
| DIP-V-15105b | Xing et al., 2019a | Juvenile | 10 | – | Overall dark diffuse brown color. |
| YLSNHM00813 | Xing et al. (this publication) | Juvenile | 8 | 4 | Primaries preserved a pale brown color with a pale band extending transversely along the basal quarter of their length; a second pale band extends transversely across the primary coverts and partly into the alular coverts. |

*A '/' indicates an uncertainty and parentheses indicate that the tract is incomplete or might be incomplete.*

sampling given how much color can vary even within a single feather (Zhang et al., 2010). Therefore, melanosome-based color research can only provide a general idea of the coloration and not a detailed reconstruction of the color patterning (Zheng et al., 2017). Furthermore, feathers in lithic specimens are typically only preserved forming a halo around the skeleton because most often a majority of the feathers are prepared away where they overlap the bones themselves. Therefore, even if all preserved feathers were sampled for SEM analysis in such specimens, the plumage color and patterns revealed would still be incomplete.

In contrast, the large-scale color patterns of light and dark areas can be observed directly in all known feathered specimens preserved in amber in which presumably the whole feather (including the keratin matrix) is preserved and not just the decay resistant melanosomes. Although also limited by incomplete preservation, in this case because only portions of the skeleton and their associated soft tissues are preserved, the detailed color patterns revealed in several complete wings preserved in amber represent a major source of data concerning plumage patterns, but perhaps not true coloration, in enantiornithines in at least one ecological environment (wet tropical forest) (Xing et al., 2018b).

Although in tropical forests today we typically envision birds that are brightly colored, in most Burmese amber specimens the feathers are preserved with various shades of brown and this base coloring is supplemented with pale markings (inferred to represent areas of reduced or absent pigmentation) (Xing et al., 2017). Observed markings include transverse bands (LV-0321, HPG-15-1, DIP-V-15101) (Xing et al., 2016, 2017, 2020), spots (LV-0321, HPG-15-1, HPG-15-2, DIP-V-15100 and DIP-V-15101) (Xing et al., 2016, 2019a,c, 2020) and possibly longitudinal stripes (LV-0321) (Xing et al., 2020). The brownish appearance of the feathers may be somewhat due to the yellow of the amber itself. The fact that all specimens known so far reveal brown coloration may additionally suggest that the color of the feathers is somehow altered by the chemistry and preservational history of the resin. While the shade of brown color itself may prove not to be reliable, the distinct spots and bands are most likely features indicative of original plumage patterning – if due to degradation, a more random pattern would be expected. Although spots and stripes have been identified in a few exceptional feathered dinosaurs from the Jehol including some birds (Chen et al., 1998; Zheng et al., 2017; Li et al., 2018) and the ornamental tail feathers in one juvenile enantiornithine from Brazil preserve unusual spots that may represent remnants of original coloring (de Souza Carvalho et al., 2015), all currently available information on plumage patterning in the wings of enantiornithines is from specimens preserved in Burmese amber (O'Connor, 2020).

The presence of pale bands and spots is not unique to YLSNHM00813. However, the combination of features present in this specimen is distinct from all previously described specimens (**Figure 5**). In HPG-15-1 the primaries are preserved with an overall walnut brown color interrupted by two transverse bands in the distal half with pale apices, while the alula feathers showed a paler color in the trailing edge vane (Xing et al., 2017; **Figure 5A**). In YLSNHM00813 the transverse pale bands are located in the basal (proximal) quarter of the remiges, not in the distal section of the feathers as in HPG-15-1, and the feather apices lack the

paler coloration, somewhat resembling the pattern in the wings of a Northern Mockingbird (*Mimus polyglottos*) (**Figure 5H**). However, these two specimens are similar in that the coverts have an overall darker pigmentation in the barbules with the rachis and barb rami being relatively paler (**Figure 4**). The feathers in the two well-preserved wings DIP-V-15100 and DIP-V-15101 have an overall darker brown coloration than that of YLSNHM00813, and show a pale spot basal to the alula (Xing et al., 2016). In DIP-V-15100, this pale spot extends on to some of the primary coverts, whereas in DIP-V-15101 a secondary pale band is also present extending across the dorsal surface of the wing apical to the alula (Xing et al., 2016). A diffuse brown coloration is present throughout the wing plumage in DIP-V-15102 and DIP-V-15105b, but the barbs have paler cores in DIP-V-15102 (Xing et al., 2018a, 2019a). The holotype of *Elektorornis chenguangi* (HPG-15-2) also preserves some wing feathers with two large-scale pale wing spots halfway down the length of the primaries, and the trailing edge vane of each primary has a pale margin (Xing et al., 2019c). Another partial wing specimen, LV-0321, consisting of the distal portion of a manus with attached primaries, preserves a pattern that is also unique from all other specimens (Xing et al., 2020). The barbs in the primaries are mostly a dark brown color, whereas the rachis is pale or white. Along the length of each primary rachis there are three patches of barbs in which the inner portions are white forming three spots on each feather that together form three transverse bands on the wing as a whole. The basal two spots somewhat grade into each other and this has been described as forming a longitudinal stripe (Xing et al., 2020).

## Ecological Implications of Observed Plumage Patterns

The plumage patterns observed in avian specimens preserved in Burmese amber have certainly been affected by taphonomic processes although to what degree is currently not understood. Interpretations regarding the plumage provided here are preliminary, and would certainly be affected by new data in the future should these specimens be subject to chemical analyses and or high resolution imaging capable of identifying additional pigments or melanic microstructure (Thomas et al., 2014). Furthermore, most of the avian specimens recovered from Burmese amber, including the specimen described here, are inferred to represent juveniles or even hatchlings and therefore the preserved plumage patterns may at least partially reflect this early ontogenetic stage and may also be subject to pronounced changes later in ontogeny. So far, all of the Burmese amber specimens appear to have generally cryptic color patterns and palettes that would have made the individuals inconspicuous in forest habitats. Solely based on this patterning, it is not possible to make absolute statements about ecology given the competing selective pressures acting on modern birds (Baker and Parker, 1979). In general, birds feeding at night, spending significant time on the ground, and or employing poorly concealed incubation sites and reduced parental care for juveniles, tend to have less conspicuous dorsal wing surface coloration (Baker and Parker, 1979). The few spots and bands of pale or white color

that are present on the Burmese enantiornithine wings also seem to be consistent with disruptive camouflage, and if they were bright white, they may have been useful in visual signaling, or predator and prey startling strategies (Jabłoński, 1996; Smithwick et al., 2017).

In comparison to modern birds, Burmese enantiornithines fall at the small end of the avian spectrum. The color patterns found in their wing feathers show a mixture of the patterns observed in extant birds from varying ecologies. Among Passeriformes, some taxa with relatively monotonous dark plumage have pale apices or bands running through their coverts, or pale spots near the alula or within the propatagium that are reminiscent of the patterns observed in amber enantiornithines. A few thrushes, grosbeaks, creepers, and warblers (e.g., *Ixoreus naevus*, *Pheucticus ludovicianus*, *Certhia americana*, and *Setophaga caerulescens*) even have broad pale bands among the primary and secondary feathers that are composed of spots similar to those in the amber specimens. However, the repetition of relatively broad pale bands in the primaries and secondaries of some amber specimens is also somewhat reminiscent of modern Falconiformes, such as kestrels (e.g., *Falco sparverius*). With the currently available data, these patterns are not clearly indicative of a particular ecology, but probably relate to crypsis. Cryptic color patterns in these juvenile enantiornithines may relate to ontogeny or to trophic ecology, since enantiornithines have been compared to raptorial birds based on their pedal morphology (O'Connor, 2019).

## CONCLUSION

The new specimen YLSNHM00813 most likely represents a juvenile enantiornithine, like a majority of previously described specimens from Burmese amber. The limb proportions differ from that of the most complete enantiornithine previously reported in amber suggesting some ecological diversity among the enantiornithines in this fauna. In all specimens the feathers are preserved with a visible brown color, suggesting this may not be indicative of *in vivo* coloration. Pale spots and bands are considered to be true features. Although obscured by preservation and other inclusions in the amber,

it appears that the plumage pattern differs in all specimens uncovered so far.

In the future, novel chemical analyses may help to further elucidate how color patterns observed in feathers preserved within amber would actually translate to *in vivo* coloration. As we gain a better understanding of these color patterns, they may eventually improve our understanding of species-level diversity in the Hukawng avifauna.

## DATA AVAILABILITY STATEMENT

All the raw data generated from the CT scans for this study are included in the MorphoSource and available at: https://www.morphosource.org/Detail/ProjectDetail/Show/project_id/1067.

## AUTHOR CONTRIBUTIONS

LX, JO'C, PC, and RM designed the project. LX, JO'C, PC, RM, KN, and HM performed the research. JO'C, PC, RM, and LX wrote the manuscript. All authors contributed to the article and approved the submitted version.

## FUNDING

## SUPPLEMENTARY MATERIAL

The Supplementary Material for this article can be found online at: https://www.frontiersin.org/articles/10.3389/feart.2020.00264/full#supplementary-material

## REFERENCES

Atterholt, J. A., Hutchison, J. H., and O'Connor, J. (2018). The most complete enantiornithine from North America and a phylogenetic analysis of the avisauridae. *PeerJ* 6:e5910. doi: 10.7717/peerj.5910

Baker, R. R., and Parker, G. A. (1979). The evolution of bird coloration. *Trans. R. Soc. Lond.* 287, 63–130. doi: 10.1098/rstb.1979.0053

Baumel, J. J., and Witmer, L. M. (1993). "Osteologia," in *Handbook of Avian Anatomy: Nomina Anatomica Avium*, Second Edition, eds J. J. Baumel, A. S. King, J. E. Breazile, H. E. Evans and J. C. Vanden Berge (Cambridge: Nuttall Ornithological Club), 45–132.

Chang, M.-M., Chen, P.-J., Wang, Y.-Q., Wang, Y., and Miao, D.-S. (eds) (2003). *The Jehol Fossils: The Emergence of Feathered Dinosaurs, Beaked Birds and Flowering Plants*. Shanghai: Shanghai Scientific & Technical Publishers.

Chen, P.-J., Dong, Z., and Zhen, S. (1998). An exceptionally well-preserved theropod dinosaur from the yixian formation of China. *Nature* 391, 147–152. doi: 10.1038/34356

Chiappe, L. M. (1993). Enantiornithine (Aves) tarsometatarsi from the cretaceous lecho formation of northwestern argentina. *Am. Museum Novit.* 3083, 1–27.

Chiappe, L. M., Ji, S., and Ji, Q. (2007). Juvenile birds from the Early cretaceous of China: implications for enantiornithine ontogeny. *Am. Museum Novit.* 3594, 1–46.

Chiappe, L. M., Liu, D., Serrano, F. J., Zhang, Y.-G., and Meng, Q.-J. (2019). Anatomy and flight performance of the early enantiornithine bird *Protopteryx fengningensis*: information from new specimens of the early cretaceous huajiying formation of China. *Anatom. Record* 303, 716–731. doi: 10.1002/ar.24322

Chiappe, L. M., and Walker, C. A. (2002). "Skeletal morphology and systematics of the cretaceous euenantiornithes (Ornithothoraces: Enantiornithes)," in *Mesozoic Birds: Above the Heads of Dinosaurs*, eds L. M. Chiappe and L. M. Witmer (Berkeley: University of California Press), 240–267.

Davies, E. H. (2001). *Palynological Analysis And Age Assignments Of Two Burmese Amber Sample Sets.* Calgary: Branta Biostratigraphy Ltd.

de Souza Carvalho, I., Novas, F. E., Agnolin, F. L., Isasi, M. P., Freitas, F. I., and Andrade, J. A. (2015). A mesozoic bird from gondwana preserving feathers. *Nat. Commun.* 6, 1–5.

Elzanowski, A. (2002). "Archaeopterygidae (upper Jurassic of Germany)," in *Mesozoic Birds: Above the Heads of Dinosaurs*, eds L. M. Chiappe and L. M. Witmer (Berkeley: University of California Press), 129–159.

Gill, F. B. (2007). *Ornithology*, 3rd Edn, New York, NY: W.H. Freeman and Company.

Grimaldi, D. A., Engel, M. S., and Nascimbene, P. C. (2002). Fossiliferous cretaceous amber from Myanmar (Burma): its rediscovery, biotic diversity, and paleontological significance. *Am. Museum Novit.* 2002, 1–71. doi: 10.1206/0003-0082(2002)361<0001:fcafmb>2.0.co;2

Hu, H., and O'Connor, J. K. (2017). First species of enantiornithes from sihedang elucidates skeletal development in early cretaceous enantiornithines. *J. Syst. Palaeontol.* 15, 909–926. doi: 10.1080/14772019.2016.1246111

Jabłoński, P. (1996). Dark habitats and bright birds: warblers may use wing patches to flush prey. *Oikos* 75, 350–352.

Ji, Q., Currie, P. J., Norell, M. A., and Ji, S.-A. (1998). Two feathered dinosaurs from northeastern China. *Nature* 393, 753–761. doi: 10.1038/31635

Li, Q.-G., Clarke, J. A., Peteya, J. A., and Shawkey, M. D. (2018). Elaborate plumage patterning in a Cretaceous bird. *PeerJ* 6:e5831. doi: 10.7717/peerj.5831

Lovette, I. J., and Fitzpatrick, J. W. (2004). *The Handbook Of Bird Biology*. New Jersey: Princeton University Press.

Lucas, S. G., and Stettenheim, P. R. (1972). *Avian Anatomy: Integument Part I*. Washington, DC: U.S. Department of Agriculture.

Martínez-Delclòs, X., Briggs, D. E. G., and Peñalver, E. (2004). Taphonomy of insects in carbonates and amber. *Palaeogeogr. Palaeoclimatol. Palaeoecol.* 203, 19–64. doi: 10.1016/S0031-0182(03)00643-646

O'Connor, J. (2012). A revised look at *Liaoningornis longidigitrus* (Aves). *Verteb. Palasiat.* 5, 25–37.

O'Connor, J. (2020). "The plumage of basal birds," in *The Evolution of Feathers*, eds C. Foth and O. W. M. Rauhut (Cham: Springer), 147–172. doi: 10.1007/978-3-030-27223-4_9

O'Connor, J. K. (2019). The trophic habits of early birds. *Palaeogeogr. Palaeoclimatol. Palaeoecol.* 513, 178–195. doi: 10.1016/j.palaeo.2018.03.006

O'Connor, J. K., Chiappe, L. M., and Bell, A. (2011). "Pre-modern birds: avian divergences in the mesozoic," in *Living Dinosaurs: the Evolutionary History of Birds*, eds G. D. Dyke and G. Kaiser (Hoboken, NJ: J. Wiley & Sons), 39–114. doi: 10.1002/9781119990475.ch3

O'Connor, J. K., Gao, K.-Q., and Chiappe, L. M. (2010). A new ornithuromorph (Aves: Ornithothoraces) bird from the Jehol group indicative of higher-level diversity. *J. Verteb. Paleontol.* 30, 311–321. doi: 10.1080/02724631003617498

O'Connor, J. K., Wang, X.-R., Chiappe, L. M., Gao, C.-H., Meng, Q.-J., Cheng, X.-D., et al. (2009). Phylogenetic support for a specialized clade of cretaceous enantiornithine birds with information from a new species. *J. Verteb. Paleontol.* 29, 188–204. doi: 10.1080/02724634.2009.10010371

Pan, Y.-H., Sha, J.-G., Zhou, Z.-H., and Fürsich, F. T. (2013). The Jehol biota: definition and distribution of exceptionally preserved relicts of a continental early cretaceous ecosystem. *Cretaceous Res.* 44, 30–38. doi: 10.1016/j.cretres.2013.03.007

Perrichot, V. (2004). Early cretaceous amber from south-western france: insight into the mesozoic litter fauna. *Geol. Acta* 2, 9–22.

Sanz, J. L., and Ortega, F. (2002). The birds from las hoyas. *Sci. Prog.* 85, 113–130. doi: 10.3184/003685002783238843

Shi, G., Grimaldi, D. A., Harlow, G. E., Wang, J., Wang, J., Yang, M., et al. (2012). Age constraint on burmese amber based on U-Pb dating of zircons. *Cretaceous Res.* 37, 155–163. doi: 10.1016/j.cretres.2012.03.014

Smithwick, F. M., Nicholls, R., Cuthill, I. C., and Vinther, J. (2017). Countershading and stripes in the theropod dinosaur sinosauropteryx reveal heterogeneous habitats in the early cretaceous Jehol biota. *Curr. Biol.* 27, 3337–3343.

Thomas, D. B., Nascimbene, P. C., Dove, C. J., Grimaldi, D. A., and James, H. F. (2014). Seeking carotenoid pigments in amber-preserved fossil feathers. *Sci. Rep.* 4, 1–6.

Wang, M., O'Connor, J., Zhou, S., and Zhou, Z.-H. (2019). New toothed early cretaceous ornithuromorph bird reveals intraclade diversity in pattern of tooth loss. *J. Syst. Palaeontol.* 18, 631–645. doi: 10.1080/14772019.2019.1682696

Wang, M., and Zhou, Z.-H. (2019). A new enantiornithine (Aves: Ornithothoraces) with completely fused premaxillae from the early cretaceous of China. *J. Syst. Palaeontol.* 17, 1299–1312. doi: 10.1080/14772019.2018.1527403

Wang, X.-L., O'Connor, J. K., Zheng, X.-T., Wang, M., Hu, H., and Zhou, Z.-H. (2014). Insights into the evolution of rachis dominated tail feathers from a new basal enantiornithine (Aves: Ornithothoraces). *Biol. J. Linnean Soc.* 113, 805–819. doi: 10.1111/bij.12313

Wright, C. W., Callomon, J. H., and Howarth, M. K. (1996). "Cretaceous ammonoidea," in *Treatise on Invertebrate Paleontology. Part I. Mollusca 4 (Revised)*, ed. R. L. Kaesler (Boulder: Geological Society of America), 362.

Xing, L.-D., McKellar, R. C., and O'Connor, J. (2020). An unusually large bird wing in mid-cretaceous burmese amber. *Cretaceous Res.* 110:104412. doi: 10.1016/j.cretres.2020.104412

Xing, L.-D., McKellar, R. C., O'Connor, J., Bai, M., Tseng, K.-W., and Chiappe, L. M. (2019a). A fully feathered enantiornithine foot and wing fragment preserved in mid-cretaceous burmese amber. *Sci. Rep.* 9, 1–9.

Xing, L.-D., McKellar, R. C., O'Connor, J. K., Niu, K.-C., and Mai, H.-J. (2019b). A mid-cretaceous enantiornithine foot and tail feather preserved in Burmese amber. *Sci. Rep.* 9, 1–8.

Xing, L.-D., O'Connor, J., Chiappe, L. M., McKellar, R. C., Carroll, N., Hu, H., et al. (2019c). A new enantiornithine with unusual pedal proportions found in amber. *Curr. Biol.* 29, 2396–2401.

Xing, L.-D., McKellar, R. C., Wang, M., Bai, M., O'Connor, J. K., Benton, M. J., et al. (2016). Mummified precocial bird wings in mid-cretaceous burmese amber. *Nat. Commun.* 7:12089.

Xing, L.-D., O'Connor, J. K., McKellar, R. C., Chiappe, L. M., Bai, M., Tseng, K.-W., et al. (2018a). A flattened enantiornithine in mid-cretaceous burmese amber: morphology and preservation. *Sci. Bull.* 63, 235–243. doi: 10.1016/j.scib.2018.01.019

Xing, L.-D., Stanley, E. L., Bai, M., and Blackburn, D. C. (2018b). The earliest direct evidence of frogs in wet tropical forests from cretaceous burmese amber. *Sci. Rep.* 8:8770.

Xing, L.-D., O'Connor, J. K., McKellar, R. C., Chiappe, L. M., Tseng, K.-W., Li, G., et al. (2017). A mid-Cretaceous enantiornithine (Aves) hatchling preserved in Burmese amber with unusual plumage. *Gondwana Res.* 49, 264–277. doi: 10.1016/j.gr.2017.06.001

Zhang, F., Zhou, Z., Hou, L., and Gu, G. (2001). Early diversification of birds: evidence from a new opposite bird. *Chin. Sci. Bull.* 46, 945–949. doi: 10.1007/bf02900473

Zhang, F.-C., Kearns, S. L., Orr, P. J., Benton, M. J., Zhou, Z.-H., Johnson, D., et al. (2010). Fossilized melanosomes and the colour of cretaceous dinosaurs and birds. *Nature* 463, 1075–1078. doi: 10.1038/nature08740

Zheng, X.-T., O'Connor, J. K., Wang, X.-L., Pan, Y.-H., Wang, Y., Wang, M., et al. (2017). Exceptional preservation of soft tissue in a new specimen of eoconfuciusornis and its biological implications. *Natl. Sci. Rev.* 4, 441–452. doi: 10.1093/nsr/nwx004

Zhou, Z., Barrett, P. M., and Hilton, J. (2003). An exceptionally preserved lower cretaceous ecosystem. *Nature* 421, 807–814. doi: 10.1038/nature01420